Available online at SciVerse ScienceDirect

SciVerse ScienceDirect

J. Mater. Sci. Technol., 2013, 29(1), 13−16

JMST

www.JMST.org

# Preparation and Characterization of $Ca_3Co_4O_9$ Thin Films on Polycrystalline $Al_2O_3$ Substrates by Chemical Solution Deposition

*Yankun Fu*[1,2], *Xianwu Tang*[1], *Jie Yang*[1], *Hongbin Jian*[1], *Xuebin Zhu*[1)*], *Yuping Sun*[1]

1) Key Laboratory of Materials Physics, Institute of Solid State Physics, Chinese Academy of Sciences, Hefei 230031, China

2) College of Science, Shandong University of Science and Technology, Qingdao 266510, China

[Manuscript received April 20, 2012, in revised form May 14, 2012, Available online 24 December 2012]

$Ca_3Co_4O_9$ thin films have been first prepared on polycrystalline $Al_2O_3$ substrates using chemical solution deposition method by multiple annealing processing. It is observed that the derived thin films are *c*-axis oriented although the substrates are polycrystalline $Al_2O_3$ substrates, suggesting the self-assembled *c*-axis orientation. The annealing temperature effects on the properties are investigated and discussed. The best performances are attributed to the 850 °C-annealed sample, whose resistivity, Seebeck coefficient and power factor at 300 K are 7.4 mΩ cm, 117 μV/K and 0.18 mW/m $K^{-2}$ respectively, which is even better than those of the thin films deposited on single crystal substrates. The results will provide an effective route to optimize the properties of $Ca_3Co_4O_9$ thin films using chemical solution deposition by multiple annealing processing even the substrates are polycrystalline.

**KEY WORDS: Chemical solution deposition; Thermoelectric; Cobaltate**

## 1. Introduction

Since relatively large Seebeck coefficient as well as small resistivity is observed in $NaCo_2O_4$[1], lots of attentions have been focused on layered cobaltates due to their rich physical properties as well as potential applications as high temperature thermoelectric (TE) materials. $Ca_3Co_4O_9$ (CCO) is a typical layered cobaltate, which consists of rock-salt $Ca_2CoO_3$ layers serving as blocking layers and triangular $CoO_2$ layers serving as conducting layers[2]. As compared with conventional high temperature TE materials such as Si−Ge alloys, the resistivity of CCO is relatively large, which should be dissolved for applications. Due to the anisotropic properties of CCO, the TE properties are more excellent along *ab* plane than along *c*-axis layer. It is necessary to fabricate *c*-axis oriented CCO materials. On the other hand, it is desirable to prepare *c*-axis oriented CCO thin films due to lots of TE applications such as thermochemistry-on-a-chip, DNA microarrays, fiber-optic switches, and microelectrothermal systems[3].

Up to now, several methods have been used successfully to prepare CCO thin films including pulsed laser deposition[4,5], sputtering[6], and chemical solution deposition (CSD)[7−12]. As compared to other methods, CSD is easy to deposit large-area thin films, to prepare thin films on complicated substrates, and to mix the precursors at atomic scale[13]. Although CCO thin films are always *c*-axis oriented despite of the orientation of the substrates, it is desirable to prepare *c*-axis oriented CCO thin films on polycrystalline substrates due to the difficulty for large-area single crystal preparation with high cost.

Here, we first report the results about CCO thin films on polycrystalline $Al_2O_3$ substrates by CSD. It is shown that the derived CCO thin films are *c*-axis oriented with relatively good performances, which suggests that polycrystalline $Al_2O_3$ substrates are suitable for preparation of *c*-axis oriented CCO thin films by CSD.

## 2. Experimental

The CCO thin films were fabricated by the simple CSD method. Briefly, calcium acetate and cobalt acetate were dissolved into propionic acid with stirring for 30 min at 70 °C. In order to obtain a well-mixed solution, the solution was stirred at room temperature for more than 10 h. The used solution concentration was adjusted to 0.2 mol/L. The thin films were deposited using a spin-coating method with the rotation speed of 4000 r/min and time of 60 s; then, the deposited thin films were baked at 400 °C for 30 min in order to expel out the organics and annealed at 750, 800 and 850 °C for 1 h under flowing oxygen atmosphere by rapid thermal annealing (RTA). The spin-coating,

* Corresponding author. Prof., Ph.D.; Tel.: +86 551 5591439; Fax: +86 551 5591434; E-mail address: xbzhu@issp.ac.cn (X. Zhu).



http://dx.doi.org/10.1016/j.jmst.2012.12.007

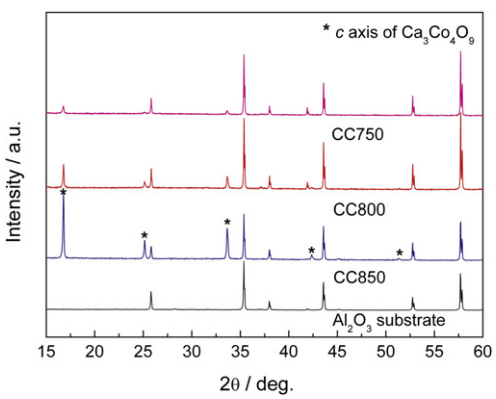


**Fig. 1** XRD results for all derived CCO thin films with polycrystalline $Al_2O_3$ substrate.

baking and annealing procedures were repeated for eight times to enhance the thickness. The CCO thin films annealed at 750, 800 and 850 °C were defined as CC850, CC800 and CC750, respectively.

The crystal phase was checked up by the X-ray diffraction (XRD, Philips X'pert Pro). The thin films morphology and thickness were determined by the field-emission scanning electron microscopy (FE-SEM, FEI Sirion 200 type, FEI, Hillsboro, OR). The resistivity was measured on a Quantum Design physical properties measurement system (PPMS) using the four point probe method and the Seebeck coefficients were also measured on the PPMS.

## 3. Results and Discussion

Fig. 1 is the XRD results for all derived thin films. It is observed that all samples show *c*-axis orientation without non-*c*-axis CCO phase and the peak intensity is enhanced with annealing temperature due to the enhanced crystalline quality. The *c*-axis lattice constant calculated using Scherrer formula is about 1.07 nm for all samples, which is similar to the bulk ceramics[2] and suggests that the oxygen content is almost same for all derived samples.

In general, for a thin film the interface energy between the substrate and the thin film plays a vital role in determination of the thin film orientation. It is unusual to observe that the derived CCO thin films are *c*-axis oriented even the substrate is polycrystalline. The driving forces for the *c*-axis orientation can be attributed to the syneresis stress due to the evaporation of organics during processing. In the case of a solution-derived film, the solvent is drawn from the film. Also, the film adheres to the substrate during the evaporation of the solvent. Therefore, the drying process gives rise to an internal stress, which is normal to the interface (*z*-direction) and can be described as an effective syneresis stress. The syneresis stress will facilitate the thin films growth along the orientation with the lowest surface energy as discussed in our previous report[7]. Also, the layered structure of the CCO with weak van der Waals bonding between two neighboring layers as well as a more stronger bonding of *c*-axis plane of CCO with $Al_2O_3$ (00l) plane than other planes[6]. That means that although the $Al_2O_3$ is polycrystalline, the CCO (00l) planes tend to nucleate onto the $Al_2O_3$ (00l) planes serving as seeds for *c*-axis oriented growth, resulting in the *c*-axis self-assembled orientation.

Fig. 2(a)−(c) is the surface FE-SEM results. It is seen that the grain size increases with increasing annealing temperature due to the enhanced crystalline quality from the enhanced atomic diffusion. The thickness is about 900 nm as determined from the cross-section FE-SEM result as shown in Fig. 2(d).

Fig. 3 is the temperature dependent resistivity, $\rho-T$. It is seen that the resistivity at 300 K ($\rho_{300\ K}$) decreases with increasing annealing temperature. The $\rho_{300\ K}$ for the CC750, CC800 and

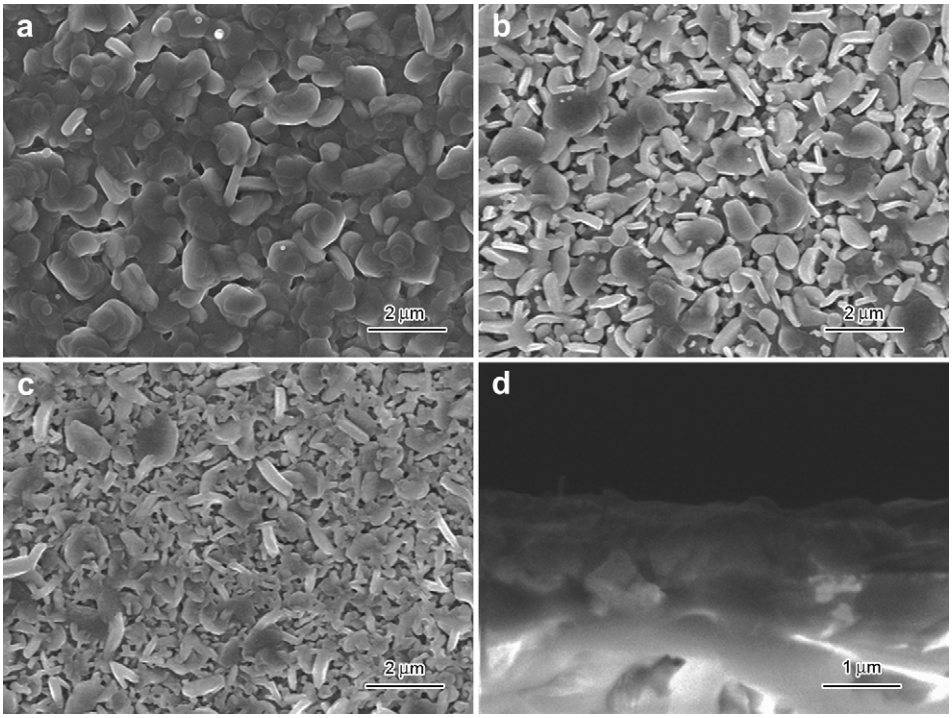


**Fig. 2** Surface FE-SEM results for all thin films: (a) CC850, (b) CC800, (c) CC750, (d) cross-section FE-SEM of CC850 for thickness measurement.

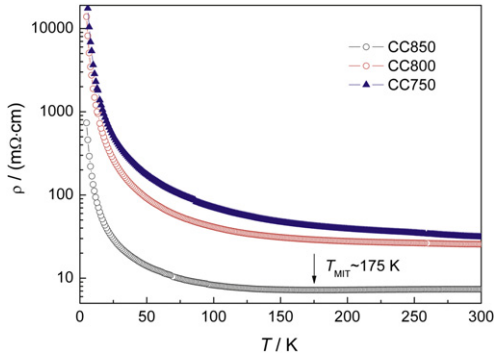


**Fig. 3** $\rho-T$ for all derived CC750, CC800 and CC850 thin films, from which it is seen that the CC850 has a MIT and the other two samples behave like semiconductors.

CC850 is 31.1, 25.6 and 7.4 mΩ cm, respectively. The similar results are also observed in the previous report about $(Ca_{2.6}Bi_{0.4})Co_4O_9$ thin films[14]. The phenomenon can be explained by the grain boundary barrier effect. The grain size and grain boundary density in polycrystalline film influence the electrical properties mainly due to carriers being scattered by the disordered atom-layers at the grain boundary. The energy barriers associated with grain boundaries can vary according to the theory of Slater[15], which is developed by Seto[16]. The barrier height $\phi$ is given by $\phi \propto (X - fL)^2$ where $X$ is the barrier width, $L$ is the dimension of the grain, and $f$ is a fraction of the order of 1/15 to 1/50. $X$ is related to the number of disordered atom-layers. Supposing that $X$ and $f$ are weakly dependent on the grain size, one can deduce that the film with the smaller grain size will have a higher barrier. The relation of carrier concentration $n$ and barrier height $\phi$ is as follows: $n \sim eQ/8\varepsilon\phi$, where $e$ is the electronic charge, $Q$ is the density of surface, and $\varepsilon$ is the dielectric permittivity[15,16]. It is the reason why the film with a smaller grain size has a larger resistivity.

Additionally, the $\rho_{300\ K}$ for CC850 is even lower than that of CCO/$SrTiO_3$ (100) thin films ($\rho_{300\ K}$ is 15.3 mΩ cm). The result suggests that the resistivity can be efficiently lowered by multiple annealing processing, which is similar to the templated induced grain growth processing. It can be also seen that the CC850 experiences a metal-insulator transition (MIT) at 175 K, which can be attributed to the localization of carriers due to the formation of incommensurate spin density wave (SDW)[17]. In order to investigate the transport properties, the $\rho-T$ result for the CC850 sample is fitted as shown in Fig. 4. It has been reported that the $\rho-T$ with MIT in CCO exhibits Fermi liquid

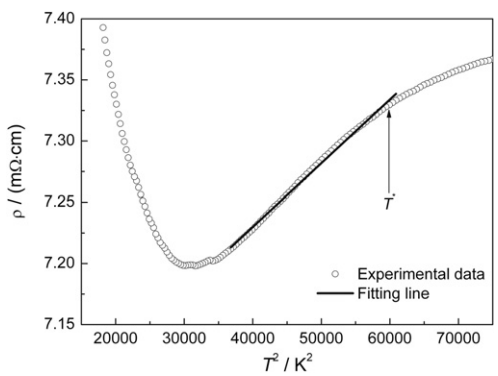


**Fig. 4** Fitting result of CC850 using the Fermi liquid theory of $\rho = \rho_0 + AT^2$.

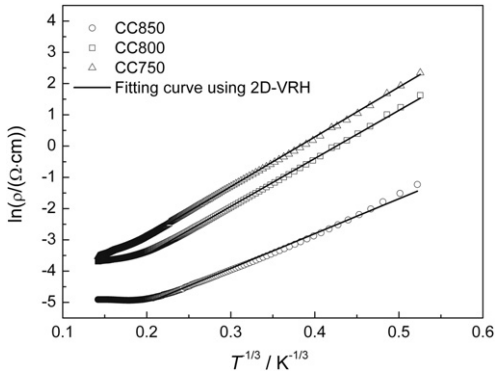


**Fig. 5** 2D-VRH fitting at low temperatures for all three samples, which suggests that the transport is dominated by 2D variable-range hopping at low temperatures.

behavior between $T_{MIT} < T < T^*$ (Mott limit temperature, $k_F l = (h/e^2)c/\rho$, with $k_F$ of Fermi wave vector and $l$ of the mean free path) with $\rho = \rho_0 + AT^2$, where $A$ is the Fermi liquid transport coefficient and $\rho_0$ is the resistivity at 0 K[18]. Beyond the $T^*$, the CCO becomes an incoherent metal (bad metal) and eventually behaves as semiconductors. The obtained values are 250 K and $\sim 1 \times 10^{-6}$ Ω cm/$K^2$ for $T^*$ and $A$, respectively. In the frame of the dynamical mean field theory (DMFT) $A \propto (m^*)^2$ and $T^* \propto 1/m^*$[19]. The enhanced $T^*$ and decreased $A$ suggest that the $m^*$ is lowered as compared to that of the CCO/$SrTiO_3$ (100) thin film. By combining with the Jonker plot as follows and the relationship of $\mu = e\tau/m^*$ ($\tau$ is the relaxation time and $\mu$ is the mobility of the carriers), it is suggested that the mobility of the carrier is enhanced due to the lowered $m^*$. The enhanced mobility will lead to the decrease of resistivity resulting in the lower resistivity for CC850 than that of the CCO/$SrTiO_3$ (100).

As for the low-temperature $\rho-T$ results, it is observed that all three samples can be well fitted using Mott's two-dimensional variable range hopping (2D-VRH) model as shown in Fig. 5[20]:

$$\rho(T) = \rho(0)\exp\left(\frac{T_0}{T}\right)^{1/3}$$

where $\rho(0)$ is a constant, $T_0$ is the VRH characteristic temperature associated with the localization length $l_v$ and the density of states $N(\varepsilon_F)$ in the vicinity of the Fermi energy level, *i.e.*, $k_B T_0 = 8/[\pi N(\varepsilon_F) l_v^2]$. The obtained $T_0$ is $\sim 4 \times 10^3$, $3.6 \times 10^3$ and $1.2 \times 10^3$ $K^3$ for CC705, CC800 and CC850, respectively. The decrease of $T_0$ with increasing

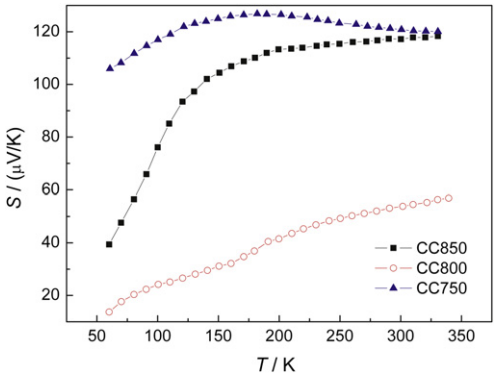


**Fig. 6** $S-T$ for all derived samples, and the positive values indicating the p-type carriers.

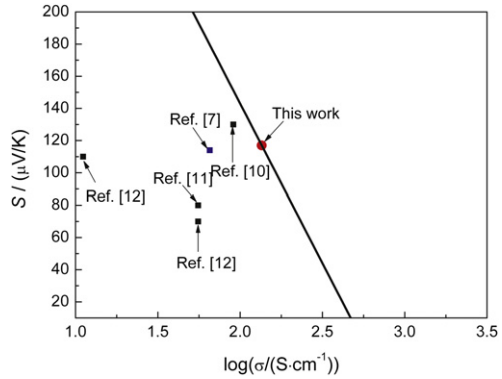


**Fig. 7** Jonker plot for the CCO thin films derived by CSD. The solid line with a slope of theoretical $S$ value (−198 μV/K) is fitted to the data point of the present film.

annealing temperature suggests the increase of localization length and enhancement of the carrier mobility, which will lead to the decrease of resistivity as observed in this experiment.

Fig. 6 is temperature dependent Seebeck coefficient ($S$−$T$) results. It is seen that the Seebeck coefficients are positive for all samples, which indicates that the major carriers are holes. Additionally, the values of the Seebeck coefficient are not changed monotonously with annealing temperature, which suggests that the simple Drude model $S \propto C/e$ with $C$ of the specific heat and $n$ of the carrier concentration cannot be used to explain the experimental results. By considering the strong correlated behaviors of the CCO material, the Mott formula $S(T) = C/n + \pi^2 k_B^2 T/3e[\partial \ln \mu(\varepsilon)/\partial \varepsilon]_{\varepsilon=E_F}$ is used to explain the experimental tendency, where $k_B$ is the Boltzmann constant and $E_F$ is the Fermi energy level[21]. When the annealing temperature is increased from 750 and 800 °C, the carrier concentration is increased, which leads to the lower resistivity and $S$ suggesting the dominant role of the first term in the Mott formula. However, when the annealing temperature is further increased to 850 °C, the second term in Mott formula will dominate resulting in the enhancement of Seebeck coefficient with the decrease of resistivity.

Fig. 7 is the Jonker plot at 300 K for CCO thin films derived by CSD method. It is seen that the data point in terms of $S$ and $\sigma$ for the present CC850 thin film is located on the right side of that of all CSD-derived CCO thin films in the Jonker plot, further confirming that the high conductivity is attributed to the enhanced carrier mobility[22].

Fig. 8 is the power factor ($PF = S^2/\rho$). It is seen that the largest $PF$ is attributed to the CC850 sample due to the lowest $\rho$ and relative large $S$, and the CC800 has the lowest $PF$ due to the lowest $S$ and relative large $\rho$. The $PF$ of the CC850 is obvious large than that of the ceramics[2], and that of the thin films prepared by CSD[7], suggesting the enhanced performances of the derived CCO thin films although the substrates are polycrystalline.

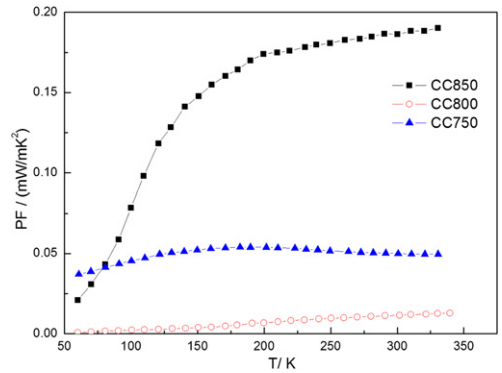


**Fig. 8** $PF$ for all three samples.

## 4. Conclusion

$c$-axis textured $Ca_3Co_4O_9$ thin films have been prepared on polycrystalline $Al_2O_3$ substrates using CSD. The annealing temperature effects on the microstructures as well as the physical properties are investigated. The resistivity, Seebeck coefficient and power factor for the 850 °C-annealed thin film is 7.4 mΩ cm, 117 μV/K and 0.18 mW/m $K^{-2}$, respectively. The results provide an effective route to prepare $c$-axis oriented CCO thin films with good performances even on polycrystalline substrates.

*Acknowledgments*

This work was supported by the National Natural Science Foundation of China (Nos. 50802096, 10904150 and 10904151).

## REFERENCES

[1] I. Terasaki, Y. Sasago, K. Uchinokura, Phys. Rev. B 56 (1997) R12685−R12687.
[2] A.C. Masset, C. Michel, A. Maigan, M. Hervieu, Phys. Rev. B 62 (2000) 166−175.
[3] R. Venkatasubramanian, E. Siivola, T. Colpitts, B. Ọquinn, Nature 413 (2001) 597−602.
[4] T. Sun, H.H. Hng, Q.Y. Yan, J. Ma, J. Appl. Phys. 108 (2010) 0837009.
[5] Y.F. Hu, W.D. Si, E. Sutter, Q. Li, Appl. Phys. Lett. 86 (2005) 082103.
[6] M. Kang, K. Cho, S. Oh, J. Kim, C. Kang, S. Nahm, S. Yoon, Appl. Phys. Lett. 98 (2011) 142102.
[7] X. Zhu, D. Shi, S. Dou, Y. Sun, Q. Li, L. Wang, W. Li, W. Yeoh, R. Zheng, Z. Chen, C. Kong, Acta Mater. 58 (2010) 4281−4291.
[8] I. Matsubara, R. Funahashi, M. Shikano, K. Sasaki, H. Enomoto, Appl. Phys. Lett. 80 (2002) 4729−4731.
[9] W. Yoon, J. Ryu, J. Choi, B. Hahn, J.H. Choi, B. Lee, J. Cho, D. Park, J. Am. Ceram. Soc. 93 (2010) 2125−2127.
[10] S. Wang, M. Chen, L. He, J. Zheng, W. Yu, G. Fu, J. Phys. D 42 (2009) 045410.
[11] L. Zhang, G.H. Liu, Y.B. Li, J.R. Xu, X.B. Zhu, Y.P. Sun, Mater. Lett. 62 (2008) 1322−1324.
[12] C. Liu, P.K. Nayak, Z. Lin, K. Jeng, Thin Solid Films 516 (2008) 8564−8568.
[13] R.W. Schwartz, Chem. Mater. 9 (1997) 2325−2340.
[14] Y. Zhou, I. Matsubara, W. Shin, N. Izu, N. Marayama, J. Appl. Phys. 95 (2004) 625−628.
[15] J.C. Slater, Phys. Rev. 103 (1956) 1631−1644.
[16] Y.W. Seto, J. Appl. Phys. 46 (1975) 5247−5254.
[17] Y. Miyazaki, K. Kudo, M. Akoshima, Y. Ono, Jpn. J. Appl. Phys. 39 (2000) L531−L533.
[18] P. Limelette, V. Hardy, P. Auban-Senzier, D. Jérome, D. Flahaut, S. Hébert, R. Frésard, Ch. Simon, J. Noudem, A. Maignan, Phys. Rev. B 71 (2005) 233108.
[19] A. Georges, G. Kotliar, W. Krauth, M.J. Rozenberg, Rev. Mod. Phys. 68 (1996) 13−125.
[20] D. Li, X.Y. Qin, Y.J. Gu, J. Zhang, J. Appl. Phys. 99 (2006) 053709.
[21] Y. Wang, Y. Sui, X. Wang, W. Su, X. Liu, J. Appl. Phys. 107 (2010) 033708.
[22] K. Sugiura, H. Ohta, K. Nomura, M. Hirano, H. Hosono, K. Koumoto, Appl. Phys. Lett. 89 (2006) 032111.